*Article*

# Stop band continuous profile filter in empty substrate integrated coaxial line

**Darío Gómez [1], Héctor Esteban [1,*], Angel Belenguer [2], Vicente E. Boria [1] and Alejandro L. Borja [2]**

1 Instituto de Telecomunicaciones y Aplicaciones Multimedia, Universitat Politècnica de València, 46022 Valencia, Spain; hesteban@dcom.upv.es
2 Departamento de Ingeniería Eléctrica, Electrónica, Automática y Comunicaciones, Universidad de Castilla-La Mancha, Escuela Politécnica de Cuenca, Campus Universitario, 16071 Cuenca, Spain; angel.belenguer@uclm.es
* Correspondence: hesteban@dcom.upv.es; Tel.: +34-96-387-7758

**Simple Summary:** A stop band continuous profile filter is implemented for the first time in the novel empty substrate integrated coaxial line technology.

**Abstract:** Substrate integrated waveguides reduce the losses and increase the quality factor of resonators in communication filters when compared with traditional planar technologies, while maintaining their low cost and low profile characteristics. Empty substrate integrated waveguides go one step further, removing the dielectric of the substrate. One of these transmission lines is the empty substrate integrated coaxial line (ESICL), which adds the advantage of being a two conductor structure. Thus, it propagates a TEM mode, which reduces the dispersion and the bandwith limitation of other one conductor empty substrate integrated waveguides. Continuous profile filters, at the cost of being long structures, are very easy to manufacture and design (usually no optimization is needed), and they are highly insensitive to manufacturing tolerances. In this work a simple continuous profile filter, with a stop band response, is designed for the first time in the novel ESICL technology. The influence of the design parameters on the insertion losses and fractional bandwidth is discussed. A prototype has been successfully manufactured and measured. A sensitivity analysis shows the high tolerance of the proposed stop band filter to manufacturing errors.

**Keywords:** Empty substrate integrated waveguides; empty substrate integrated coaxial line; ESICL; continuous profile filters; stop band filters

## 1. Introduction

The current growth of wireless communications, due to the increase in voice, video and data services, is causing a growing demand for channels and bandwidth. This is driving the future communication systems towards higher frequencies, evidencing the need for the development of such communications systems. Therefore, the aim is to develop low-cost, high-performance technology suitable for mass production, while at the same time achieving a significant reduction in the volume, weight and cost of telecommunications equipment.

Over the last years, a great number of substrate integrated circuits [1] has been developed. These circuits are a compromise between the advantages of classical waveguide technologies, such as high quality factor of resonators and low insertion losses, and the advantages of planar circuits, such as low cost and easy compact integration. The substrate integrated waveguide (SIW) [2] and the substrate integrated coaxial line (SICL) [3], are two proposals of substrate integrated circuits that have been a great advance in this field. Several passive components developed in these technologies, including filters [4,5], antennas [6,7], transitions and tapers [8,9], baluns [10,11], couplers [12,13], power dividers [14], and new transmission lines [3,15–18], have been proposed. But although their quality factor and

Preprints (www.preprints.org) | NOT PEER-REVIEWED | Posted: 7 October 2018 doi:10.20944/preprints201810.0122.v1

Peer-reviewed version available at Appl. Sci. 2018, 8, 2176; doi:10.3390/app8112176



losses are better than those of the planar circuits, these characteristics can be further improved (without losing compactness and low cost manufacturing) if the dielectric substrate is removed and the waves are allowed to propagate through air.

This is the purpose of some empty substrate integrated waveguides that have been recently proposed, such as the Modified SIW (MSIW) [19], the Empty SIW (ESIW) [20], the Air-filled SIW (AFSIW) [21], the Hollow SIW (HSIW) [22], or the Dielectricless SIW (DSIW) [23]. All these new transmission lines are integrated in a substrate and they are low profile, low cost, and with higher quality factor and less losses than the SIW, thanks to the complete or partial removal of the dielectric in the path of the electromagnetic (EM) fields. However, these are one conductor structures, which means that the fundamental mode is dispersive, and with a cut-off frequency greater than zero, which limits the usable bandwidth of microwave devices implemented with such novel technologies.

These limitations can be overcome with the use of the empty substrate integrated coaxial line (ESICL). The structure of ESICL was first used in [24] for feeding an antenna, and definitely integrated in a planar circuit in [25], where a transition to a classical planar line (a grounded coplanar waveguide) was proposed for the first time. The ESICL is a two-conductor transmission line, whose cross section is a rectangular coaxial built with the superposition of five layers of printed circuit board, as shown in Figure 1. This novel transmission line has been recently proposed, and up to date it has only been applied to the implementation of wide band [25] and narrow band [26] microwave filters with a non-dispersive TEM propagating mode. There is, consequently, many possible applications that remain to be explored for this novel transmission line.

One of these possible applications is implementing continuous profile filters. Conversely to conventional microwave filter topologies, where the filtering structure is based on sharp changes in the cross section that produce sharp impedance steps, continuous profile filters use a progressive and smooth variation of the cross section. This continuous variation has the advantage, at the cost of increasing the length of the filter, of providing a structure with much more resilience to manufacturing tolerances. Besides, the continuous profile filters can be easily and accurately designed with well-known techniques such as the ones described in [27] and [28]. All these techniques require that the phase constant is kept constant (for the same frequency) along the propagation direction. This can be achieved with a structure that propagates a TEM mode (as it is the case of the ESICL), or either with a structure that propagates a non-TEM mode and that varies the cross section along the propagation direction in such a way that the cutoff frequency of this mode does not change. This can be achieved, for instance, varying the height of a rectangular waveguide. If we vary the width of the rectangular waveguide, the cutoff frequency changes and then this is not suitable for the traditional synthesis techniques developed for continuous profile filters. Most one conductor substrate integrated transmission lines (SIW, ESIW, AFSIW, etc.) are H-plane structures, where the width of the rectangular cavity can be changed, but the height is fixed in all the structure (the height of the substrate). Some efforts have been already made to apply the traditional synthesis technique for continuous profile filters in H-plane structures (SIW filter) in [29] and [30]. Although good results are obtained, the synthesis does not provide so accurate results as when the phase constant does not change along the propagation direction. For that reason, ESICL, with a TEM propagating mode, is an excellent candidate to implement continuous profile filters in substrate integrated waveguide technology (with lower losses than both in planar and classical SIW technologies).

In this work a simple continuous profile filter is implemented in ESICL for the first time. The variation of the filter response with the design parameters is studied. A prototype is successfully manufactured and measured, and a sensitivity analysis is performed in order to test the resilience to manufacturing tolerances of this type of filter in this novel transmission line.

Preprints (www.preprints.org) | NOT PEER-REVIEWED | Posted: 7 October 2018 doi:10.20944/preprints201810.0122.v1

Peer-reviewed version available at Appl. Sci. 2018, 8, 2176; doi:10.3390/app8112176



## 2. Materials and Methods

### 2.1. ESICL

The ESICL topology can be seen in Figure 1. Figure 1.(a) shows the five substrate layers needed to manufacture the ESICL. These layers are the top and bottom metallic covers (layers 1 and 5), the central layer with the inner conductor of the ESICL (layer 3), and two more layers that separate the central layer from the top and bottom covers (layers 2 and 4). Layer 3 also hosts the transition from ESICL to the input and output planar accessing lines (coplanar or microstrip).

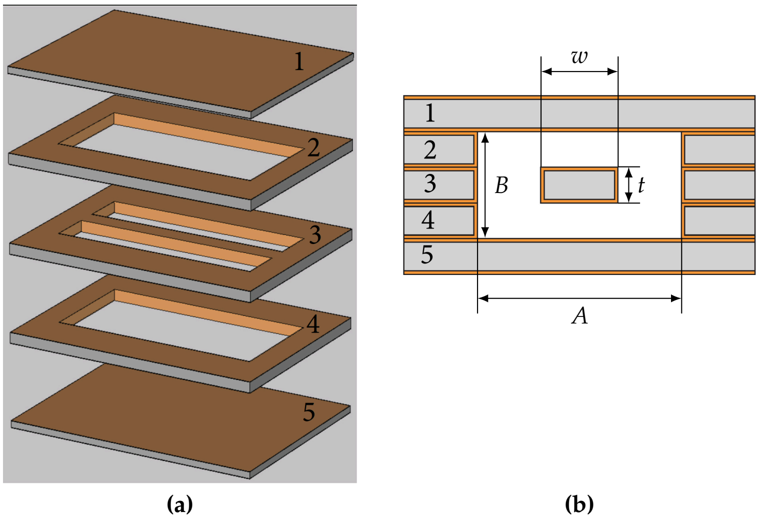


**Figure 1.** Simplest construction of an ESICL (source [25]). Layer 1 and 5 are top and bottom covers; layer 3 is the central layer with transitions to planar lines; layers 2 and 4 separate central layer from covers. **(a)** 3-D view of layers before assembling. **(b)** Cross-section of the ESICL after assembling.

The cross section of the ESICL, after the five layers are assembled and pasted with tin soldering paste together, is depicted in Figure 1.(b). As it can be observed, after assembling, the cross section is the same as that of a rectangular coaxial line, without any dielectric between the inner and the outer conductors. The dimensions of the cross section are included in the layout. These dimensions are the width ($w$) and height ($t$) of the inner conductor, and the width ($A$) and height ($B$) of the outer conductor.

### 2.2. Coupling coefficient and impedance

As it was already demonstrated in [30], a sinusoidal modulation in the profile of a transmission line produces a stop band filter response. Using the coupled-mode theory, as proposed in [31], a full analytical synthesis can be achieved. To do so, the desired frequency response is used in order to determine the variation of the coupling coefficient $K(z)$ along the propagation direction ($z$) that provides that response. For complex responses, the coupling coefficient $K(z)$ can be obtained using the zeros and poles of a ideal frequency response expressed as a rational function of polynomials, as proposed in [27]. However, for a simple response as a stop band filter, the coupling coefficient can be directly expressed as a sinusoidal variation of the form [29]:

$$K(z) = A_k \sin\left(\frac{2\pi}{\Lambda} z + \theta\right), \quad z \in [0, \ n_p \cdot \Lambda] \tag{1}$$

where $A_k$ represents the oscillation amplitude, $\Lambda$ is its period, $z$ is the propagation direction, and $\theta$ is the phase of the sinusoidal. $\theta$ should be set to 0 in order to facilitate the subsequent manufacturing process, avoiding sharp changes in the profile at the beginning of the filter.

Preprints (www.preprints.org) | NOT PEER-REVIEWED | Posted: 7 October 2018 doi:10.20944/preprints201810.0122.v1

Peer-reviewed version available at Appl. Sci. 2018, 8, 2176; doi:10.3390/app8112176



The value of $\Lambda$ controls the central frequency of the stop band. If we want to locate the center of the stop band at a certain frequency $f_0$, the period $\Lambda$ should be:

$$\Lambda = \frac{\pi}{\beta_0} \tag{2}$$

where $\beta_0$ is the phase constant of the propagating mode at the central frequency $f_0$.

The amplitude $A_k$ and the length (or number of periods $n_p$) of the sinusoidal variation of $K(z)$ control the depth of the rejection (insertion losses $IL$ at $f_0$) and the fractional bandwidth of the stop band ($FBW$), as it is described in section 2.4.

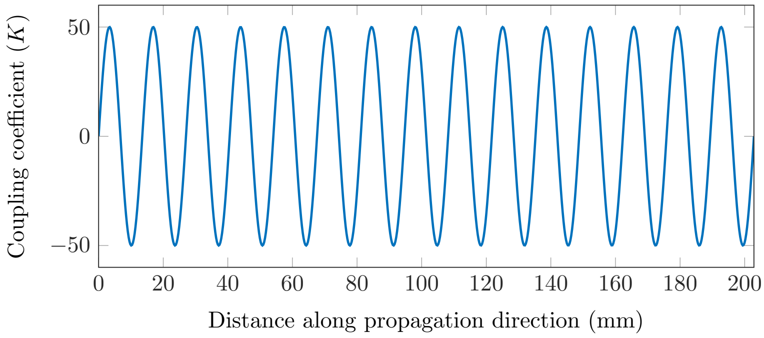


**Figure 2.** Variation of the coupling coefficient ($K(z)$) along the propagation direction ($\Lambda = 13.52$ mm, $A_k = 50$, $n_p = 15$ and $\theta = 0$).

Figure 2 shows the variation of the coupling coefficient $K(z)$ for $\Lambda = 13.52$ mm, $A_k = 50$, $n_p = 15$ and $\theta = 0$. The value of $\Lambda$ has been calculated using $\beta_0 = 232.3$ rad/m, which is the phase constant of an ESICL with $Z_0 = 50\,\Omega$ ($A = 6$ mm, $B = 2.618$ mm, $t = 0.866$ mm and $w = 1.8148$ mm) at $f_0 = 11$ GHz.

For a device propagating a TEM mode, the relationship between the coupling coefficient and the impedance along the propagation direction is [31]:

$$K = -\frac{1}{2}\frac{1}{Z_0}\frac{dZ_0}{dz} \tag{3}$$

This equation can be used to express the impedance $Z_0$ as a function of the coupling coefficient as:

$$Z_0(z) = Z_0(0)e^{-2\int_0^z K(r)dr} \tag{4}$$

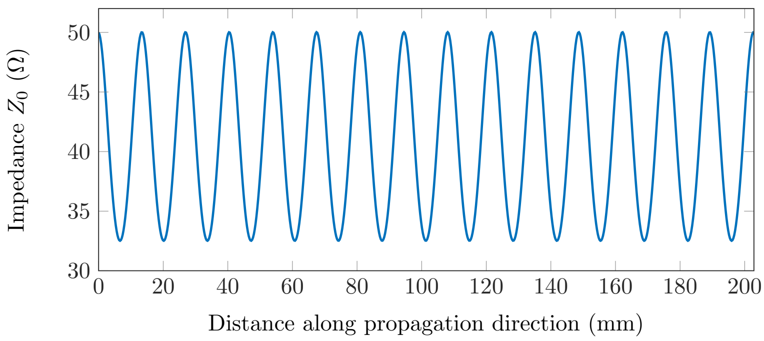


**Figure 3.** Variation of the impedance ($Z_0$) along the propagation direction.

Substituting the coupling coefficient of Figure 2 into (4), gives the impedance variation of Figure 3. The next step is to obtain an ESICL with a profile that provides this impedance variation.

Preprints (www.preprints.org) | NOT PEER-REVIEWED | Posted: 7 October 2018 doi:10.20944/preprints201810.0122.v1

Peer-reviewed version available at Appl. Sci. 2018, 8, 2176; doi:10.3390/app8112176



### 2.3. Impedance in ESICL

The impedance $Z_0$ of an ESICL depends on the dimensions of the cross section ($A$, $B$, $t$ and $w$). The following approximation for the impedance can be found in [32]:

$$Z_0 = \frac{\eta_0}{4\sqrt{\epsilon_r}} \left[ \frac{1}{\frac{w/B}{B/t-1} + \frac{2}{\pi} \ln \left( \frac{1}{1-t/B} + \coth \frac{\pi A}{2B} \right)} \right] (\Omega) \tag{5}$$

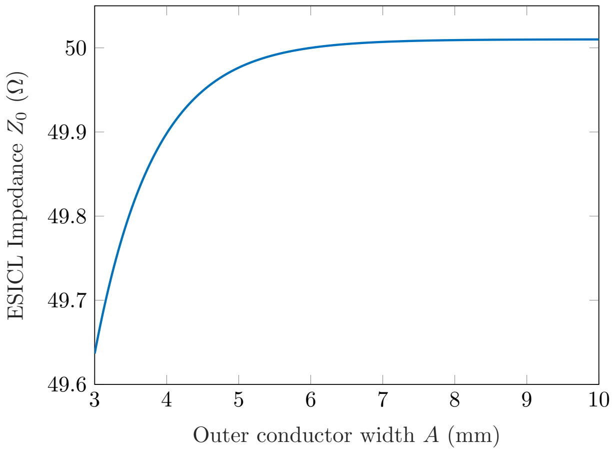


**Figure 4.** Variation of the impedance ($Z_0$) of the ESICL as a function of the outer conductor width. $B = 2.618$ mm, $w = 2.2823315$ mm, $t = 0.866$ mm. The analytic formula of (5) has been used.

In the ESICL, the heights of the inner and outer conductor are fixed by the height of the substrate layers. In this work all substrate layers will be Rogers 4003C substrates of height $h = 0.813$ mm plus electrodeposited copper foils of 17 $\mu$m. Taking also into account the thickness of the soldering paste, it gives that $t = 0.866$ mm and $B = 2.618$ mm. From (5), it can be derived that $Z_0$ does not change significantly with the width of the outer conductor $A$. Figure 4 shows the variation of $Z_0$ with $A$ using (5), and fixing the other dimensions of the cross section. It can be observed that for $A \geq 6$ mm, the impedance is almost constant. So $A$ is fixed to 6 mm, and once $A$, $B$ and $t$ are fixed, $Z_0$ depends only on the width of the inner conductor $w$.

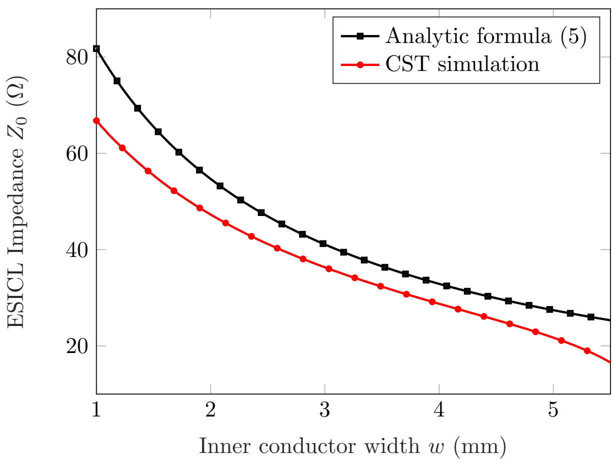


**Figure 5.** Variation of the impedance ($Z_0$) of the ESICL as a function of the inner conductor width. $B = 2.618$ mm, $A = 6$ mm, $t = 0.866$ mm. Comparison between analytic formula of (5) and simulation with CST EM solver.

 doi:10.20944/preprints201810.0122.v1

Peer-reviewed version available at Appl. Sci. 2018, 8, 2176; doi:10.3390/app8112176



Figure 5 shows the variation of $Z_0$ with $w$, while $A$, $B$ and $t$ are fixed. This impedance has been calculated with the analytic formula of (5), and also with a commercial electromagnetic solver (CST Studio). Both results are not in good agreement, so the most accurate results of the full-wave commercial simulator have been considered.

It must be noted that in order to implement the stop band filter we need an impedance variation along the propagation direction as shown in Figure 3. That is, we must be able of changing the impedance in a range from approximately 32 to 50 Ω. As shown in Figure 5, changing $w$ from 1 to 5.5 mm we can change $Z_0$ in a range that goes from 17 to 66 Ω, which is enough for implementing the stop band filter.

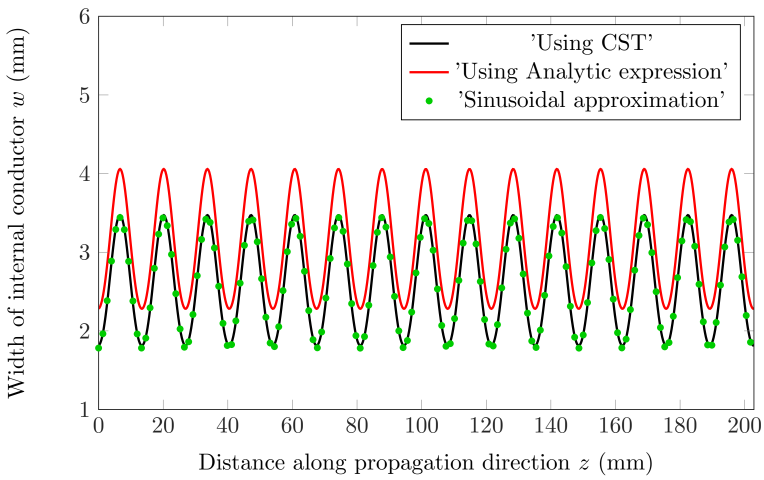


**Figure 6.** Width of the internal conductor of the ESICL ($w$) that provides the desired coupling coefficient.

Using the relationship between $Z_0$ and $w$ obtained with CST and shown in Figure 5, we can now derive the variation of the inner conductor width $w(z)$ needed to achieve the variation of the impedance $Z_0(z)$ of Figure 3 that provides the desired coupling coefficient $K(z)$, and therefore, the desired stop band response. Figure 6 shows this variation $w(z)$ for three different cases. In the first place, the value of $w(z)$ derived using the analytic formula, which has proven to be inaccurate, is plotted with a solid red line. Next, the accurate value of $w(z)$ computed with the impedance obtained with CST is plotted in solid black line. And finally, a sinusoidal approximation to the accurate value of $w(z)$ is plotted in green round marks. This approximation is calculated using the following expression:

$$w = A_w \cos\left(\frac{2\pi z}{Z_p} + P\right) - B_w \tag{6}$$

An optimization process with the Nelder Mead simplex algorithm [33] determines after 450 iterations the optimum values of the parameters $A_w$, $B_w$ and $P$ for an optimum match of this sinusoidal approximation with the accurate value of $w(z)$. It gives $A_w = 0.8305$, $B_w = 2.61103$ and $P = -3.0817$. This approximation, which matches almost perfectly the accurate value, is preferred to the accurate one, because it eases the modeling and simulation of the ESICL continuous profile filter in the electromagnetic simulator (see Figure 7 and 8).

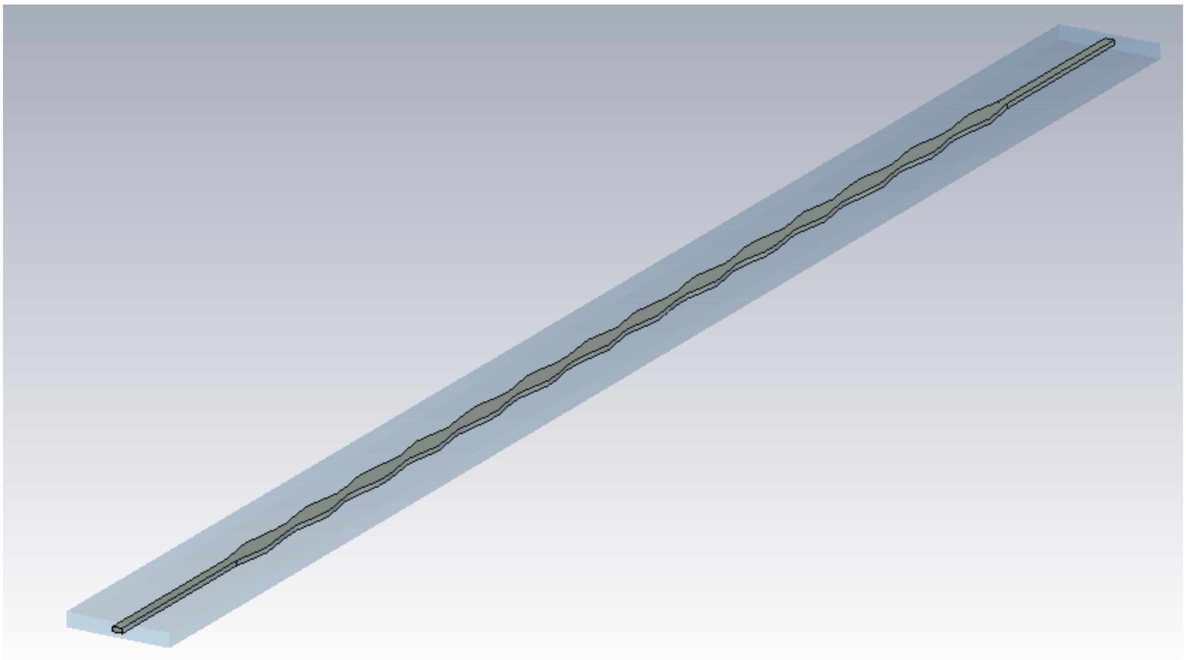

**Figure 7.** 3D model of the ESICL filter in the electromagnetic simulator (CST).

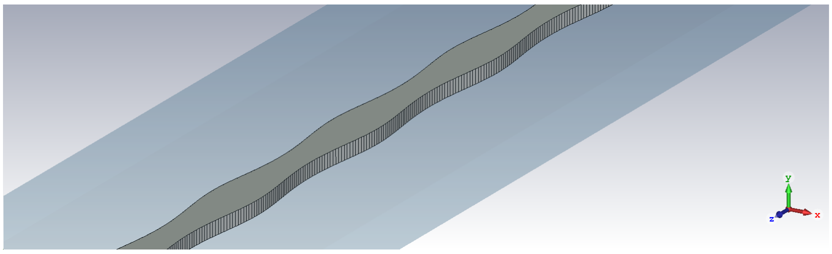

**Figure 8.** Zoom of the inner conductor in the 3D model of the EM simulator.

### *2.4. Design procedure*

The stop band response is characterized by the central frequency ($f_0$), the fractional bandwidth ($FBW$), and the insertion losses ($IL$) at the central frequency. These characteristics are determined by the amplitude ($A_k$), period ($\Lambda$), and length (number of periods $n_p$) of the sinusoidal variation of the coupling coefficient along the propagation direction (see equation (1)).

As already discussed in previous sections, the central frequency can be directly adjusted with the period $\Lambda$ using (2).

The challenge is to determine the adequate value of $A_k$ and $n_p$ in order to accomplish with the specifications of $IL$ and $FBW$.

In order to have an insight into the influence of $A_k$ and $n_p$ in the values of $IL$ and $FBW$, several simulations have been performed in CST for the ESICL filter for a discrete number of values of $A_k$ and $n_p$ with $A_k$ ranging from 10 to 80, and $n_p$ ranging from 5 to 30. And the $IL$ and $FBW$ has been computed in all possible combinations of $A_k$ and $n_p$. In all cases $\Lambda$ was selected to provide a stop band response centered at 11 GHz. The results are depicted in Figure 9.

 doi:10.20944/preprints201810.0122.v1

Peer-reviewed version available at Appl. Sci. 2018, 8, 2176; doi:10.3390/app8112176



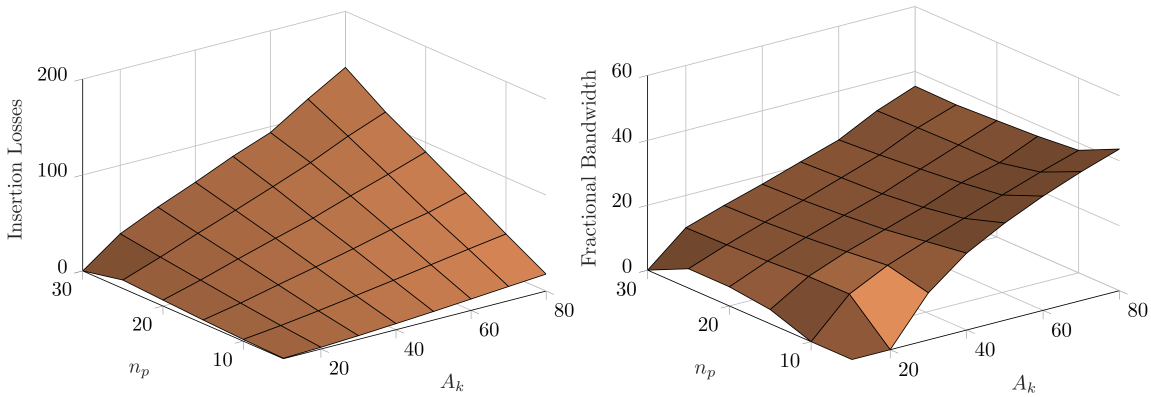


**Figure 9.** Influence of the design parameters ($A_k$ and $n_p$) in the stop band response of the ESICL filter (insertion losses and fractional bandwidth).

As it can be observed, when $A_k$ is increased, the $IL$ and the $FBW$ are both increased. And when $n_p$ is increased, the $IL$ increase, and the $FBW$ does not change significantly. This information can be useful to either perform a manual design, or either to properly decide the initial point for a computer aided optimization process that optimizes the values of $A_k$ and $n_p$ until the specifications are met.

## 3. Results

A prototype of the ESICL continuous profile filter has been manufactured and measured. The filter has been designed to have the stop band centered at 11 GHz. This leads to $\Lambda = 13.52$ mm. For the sinusoidal variation of the coupling coefficient, the values $A_k = 50$, $n_p = 15$ and $\theta = 0$ have been used, which are the values used in section 2. Therefore, the coupling coefficient is the one depicted in Figure 2, the variation of the impedance is the one shown in Figure 3, and the width of the inner conductor is the one plotted in Figure 6. The other dimensions of the ESICL cross section are $B = 2.618$mm, $A = 6$mm, $t = 0.866$ mm. With all these values, the simulated insertion losses at the central frequency are 37.8 dB, and the fractional bandwidth is 23.8%.

The prototype is manufactured with Rogers 4003C substrates of height $h = 0.813$ mm, with electrodeposited copper foils of 17 $\mu$m, and substrate permittivity $\varepsilon_r = 3.55$.

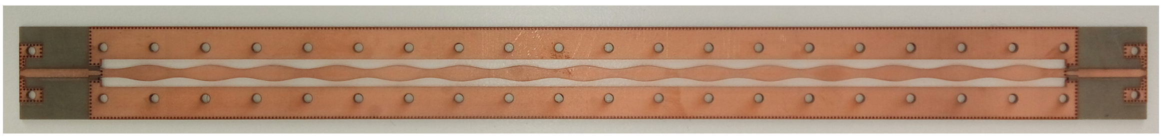

**Figure 10.** Manufactured prototype of the ESICL continuous profile filter.

The manufactured prototype is shown in Figure 10. The manufacture of the ESICL filter follows standard processes of planar circuit manufacturing (drilling, milling, and electrodeposition). First the ESICL via holes are drilled and the lateral walls are cut. Then, the substrate is metallized using electroplating. This metallizes the via holes and the lateral walls. Next the accessing planar lines and the transitions are milled. Finally, all the layers are piled together using alignment screws, and soldered using tin soldering paste. An LPKF Protolaser U3 circuit board plotter has been used for drilling, cutting and milling. An LPKF Mini Contac RS through-hole electroplating system has been used for electroplating, and an LPKF ProtoFlow S reflow oven has been used for curing the tin soldering paste.

Preprints (www.preprints.org) | NOT PEER-REVIEWED | Posted: 7 October 2018 doi:10.20944/preprints201810.0122.v1

Peer-reviewed version available at Appl. Sci. 2018, 8, 2176; doi:10.3390/app8112176



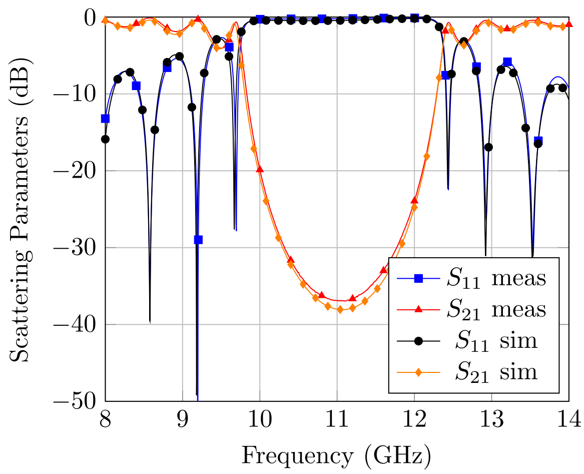


**Figure 11.** Simulated and measured scattering parameters of the manufactured ESICL filter prototype.

Figure 11 compares the simulated and measured scattering parameters of the ESICL prototype. As it can be observed, there is a very good agreement between simulation and measurements.

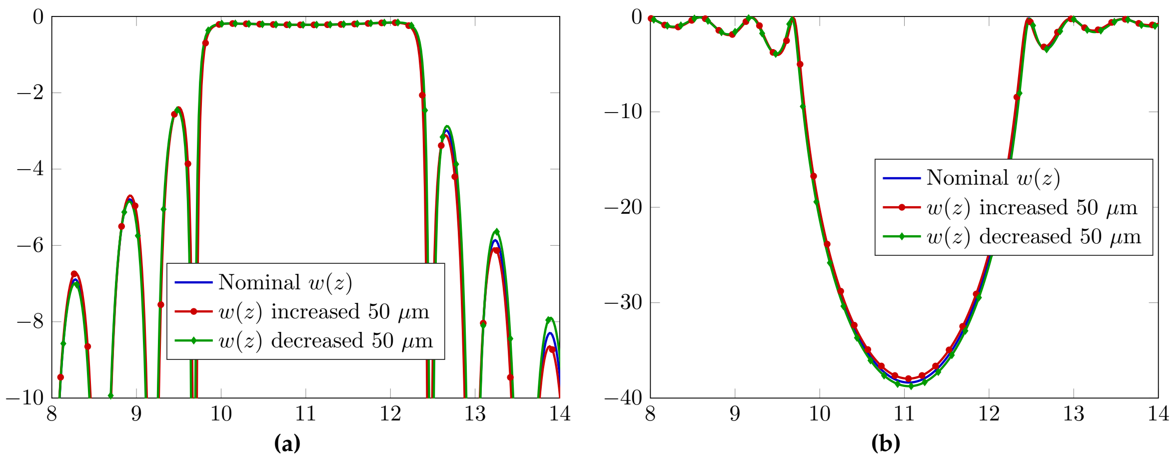


**Figure 12.** Sensitivity analysis. Comparison between scattering parameters of the filter with nominal value of the width of the inner conductor of the ESICL ($w(z)$), and with the width increased and decreased the manufacturing tolerance (50 $\mu$m). **(a)** Reflection. **(b)** Transmission.

One of the advantages of the continuous profile filters is supposed to be the high tolerance to manufacturing errors. In order to verify this low sensitivity to variations in the dimensions of the filter, the scattering parameters of the ESICL prototype have been simulated altering the width on the inner conductor ($w(z)$). This dimension is the most critical dimension of the filter, since this is the dimension that has a greater influence on the impedance of the ESICL. Taking into account the manufacturing tolerance of the machine used for drilling and cutting (50 $\mu$m), the scattering parameters have been simulated with the nominal value of $w(z)$, with $w(z)$ increased by 50 $\mu$m, and with $w(z)$ decreased by 50 $\mu$m. Results are shown in Figure 12. As it can be observed, the response of the filter does not change significantly either increasing or decreasing $w(z)$, which is consistent with the alleged advantage of this type of filters.

## 4. Discussion

In this work a stop band continuous profile filter has been implemented for the first time in ESICL. The use of ESICL has the advantages of being low cost and low profile, manufactured with

Preprints (www.preprints.org) | NOT PEER-REVIEWED | Posted: 7 October 2018 doi:10.20944/preprints201810.0122.v1

Peer-reviewed version available at *Appl. Sci.* **2018**, *8*, 2176; doi:10.3390/app8112176



standard planar circuits machinery. It has lower insertion losses and higher quality factors than planar circuits, and than substrate integrated waveguides filled with dielectric. Besides, since ESICL has two conductors, it propagates a fundamental TEM mode and has lower dispersion and higher usable bandwidth, being therefore suitable for implementing highly accurate design procedures for continuous profile filters. In this work a very simple continuous profile filter has been designed and manufactured. The influence of the design parameters on the frequency response has been studied. Measurements are in good agreement with simulations. A sensitivity analysis has been performed, proving that the structure has very high resilience to manufacturing errors. The results are promising for the extension of the ESICL to the implementation of other low cost and high quality communication devices.

**Author Contributions:** Conceptualization, H. Esteban, A. Belenguer and A. Lucas; Methodology, D. Gómez and H. Esteban; Software, D. Gómez; Formal analysis, D. Gómez and H. Esteban; Validation, A. Belenguer and A. Lucas; Investigation, D. Gómez, H. Esteban, A. Belenguer and A. Lucas; Resources, A. Belenguer, H. Esteban and V. E. Boria; Writing—Original Draft Preparation, D. Gómez; Writing—Review & Editing, H. Esteban; Visualization, D. Gómez; Supervision, H. Esteban; Project Administration, A. Belenguer and V. E Boria; Funding Acquisition, A. Belenguer and V. E. Boria

**Funding:** This research was funded by *Ministerio de Economía, Industria y Competitividad*, Spanish Government, under Research Projects TEC2016- 75934-C4-3-R and TEC2016-75934-C4-1-R.

**Conflicts of Interest:** The authors declare no conflict of interest. The founding sponsors had no role in the design of the study; in the collection, analyses, or interpretation of data; in the writing of the manuscript, and in the decision to publish the results.

## Abbreviations

The following abbreviations are used in this manuscript:

| | |
|---|---|
| SIW | Substrate integrated waveguide |
| ESIW | Empty substrate integrated waveguide |
| MSIW | Modified substrate integrated waveguide |
| AFSIW | Air filled substrate integrated waveguide |
| HSIW | Hollow substrate integrated waveguide |
| DSIW | Dielectricless substrate integrated waveguide |
| ESICL | Empty substrate integrated coaxial line |
| SICL | Substrate integrated coaxial cine |
| GCPW | Grounded coplanar waveguide |
| TEM | Transversal electric and magnetic |
| CST | Computer Simulation Technology |
| IL | Insertion losses |
| FBW | Fractional bandwidth |

## References

1. Deslandes, D.; Wu, K. Integrated microstrip and rectangular waveguide in planar form. *IEEE Microwave and Wireless Components Letters* **2001**, *11*, 68–70. doi:10.1109/7260.914305.
2. Deslandes, D.; Wu, K. Accurate modeling, wave mechanisms, and design considerations of a substrate integrated waveguide. *IEEE Transactions on Microwave Theory and Techniques* **2006**, *54*, 2516–2526. doi:10.1109/TMTT.2006.875807.
3. Gatti, F.; Bozzi, M.; Perregrini, L.; Wu, K.; Bosisio, R.G. A Novel Substrate Integrated Coaxial Line (SICL) for Wide-Band Applications. 2006 European Microwave Conference, 2006, pp. 1614–1617. doi:10.1109/EUMC.2006.281409.
4. Zhang, D.D.; Zhou, L.; Wu, L.S.; Qiu, L.F.; Yin, W.Y.; Mao, J.F. Novel Bandpass Filters by Using Cavity-Loaded Dielectric Resonators in a Substrate Integrated Waveguide. *IEEE Transactions on Microwave Theory and Techniques* **2014**, *62*, 1173–1182. doi:10.1109/TMTT.2014.2314677.

5. Chu, P.; Hong, W.; Dai, L.; Tang, H.; Chen, J.; Hao, Z.; Zhu, X.; Wu, K. A Planar Bandpass Filter Implemented With a Hybrid Structure of Substrate Integrated Waveguide and Coplanar Waveguide. *IEEE Transactions on Microwave Theory and Techniques* **2014**, *62*, 266–274. doi:10.1109/TMTT.2013.2294861.
6. Yang, T.Y.; Hong, W.; Zhang, Y. Wideband Millimeter-Wave Substrate Integrated Waveguide Cavity-Backed Rectangular Patch Antenna. *IEEE Antennas and Wireless Propagation Letters* **2014**, *13*, 205–208. doi:10.1109/LAWP.2014.2300194.
7. Liu, J.; Jackson, D.R.; Long, Y. Substrate Integrated Waveguide (SIW) Leaky-Wave Antenna With Transverse Slots. *IEEE Transactions on Antennas and Propagation* **2012**, *60*, 20–29. doi:10.1109/TAP.2011.2167910.
8. Caballero, E.D.; Martinez, A.B.; Gonzalez, H.E.; Belda, O.M.; Esbert, V.B. A novel transition from microstrip to a substrate integrated waveguide with higher characteristic impedance. 2013 IEEE MTT-S International Microwave Symposium Digest (MTT), 2013, pp. 1–4. doi:10.1109/MWSYM.2013.6697773.
9. Deslandes, D. Design equations for tapered microstrip-to-Substrate Integrated Waveguide transitions. 2010 IEEE MTT-S International Microwave Symposium, 2010, pp. 704–707. doi:10.1109/MWSYM.2010.5517884.
10. Zhang, Z.Y.; Wu, K. A Broadband Substrate Integrated Waveguide (SIW) Planar Balun. *IEEE Microwave and Wireless Components Letters* **2007**, *17*, 843–845. doi:10.1109/LMWC.2007.910479.
11. Zhu, F.; Hong, W.; Chen, J.X.; Wu, K. Ultra-Wideband Single and Dual Baluns Based on Substrate Integrated Coaxial Line Technology. *IEEE Transactions on Microwave Theory and Techniques* **2012**, *60*, 3062–3070. doi:10.1109/TMTT.2012.2209448.
12. Ali, A.; Aubert, H.; Fonseca, N.; Coccetti, F. Wideband two-layer SIW coupler: design and experiment. *Electronics Letters* **2009**, *45*, 687–689. doi:10.1049/el.2009.0464.
13. Patrovsky, A.; Daigle, M.; Wu, K. Coupling mechanism in hybrid SIW–CPW forward couplers for millimeter-wave substrate integrated circuits. *IEEE Transactions on Microwave Theory and Techniques* **2008**, *56*, 2594–2601.
14. Gatti, F.; Bozzi, M.; Perregrini, L.; Wu, K.; Bosisio, R.G. A new wide-band six-port junction based on substrate integrated coaxial line (SICL) technology. MELECON 2006 - 2006 IEEE Mediterranean Electrotechnical Conference, 2006, pp. 367–370. doi:10.1109/MELCON.2006.1653115.
15. Xu, F.; Wu, K. Substrate Integrated Nonradiative Dielectric Waveguide Structures Directly Fabricated on Printed Circuit Boards and Metallized Dielectric Layers. *IEEE Transactions on Microwave Theory and Techniques* **2011**, *59*, 3076–3086. doi:10.1109/TMTT.2011.2168969.
16. Hong, W.; Liu, B.; Wang, Y.; Lai, Q.; Tang, H.; Yin, X.X.; Dong, Y.D.; Zhang, Y.; Wu, K. Half Mode Substrate Integrated Waveguide: A New Guided Wave Structure for Microwave and Millimeter Wave Application. 2006 Joint 31st International Conference on Infrared Millimeter Waves and 14th International Conference on Teraherz Electronics, 2006, pp. 219–219. doi:10.1109/ICIMW.2006.368427.
17. Cassivi, Y.; Wu, K. Substrate integrated nonradiative dielectric waveguide. *IEEE Microwave and Wireless Components Letters* **2004**, *14*, 89–91. doi:10.1109/LMWC.2004.824808.
18. Deslandes, D.; Bozzi, M.; Arcioni, P.; Wu, K. Substrate integrated slab waveguide (SISW) for wideband microwave applications. IEEE MTT-S International Microwave Symposium Digest, 2003, 2003, Vol. 2, pp. 1103–1106 vol.2. doi:10.1109/MWSYM.2003.1212561.
19. Ranjkesh, N.; Shahabadi, M. Reduction of dielectric losses in substrate integrated waveguide. *Electronics Letters* **2006**, *42*, 1230–1231. doi:10.1049/el:20061870.
20. Belenguer, A.; Esteban, H.; Boria, V. Novel Empty Substrate Integrated Waveguide for High-Performance Microwave Integrated Circuits. *Microwave Theory and Techniques, IEEE Transactions on* **2014**, *62*, 832–839. doi:10.1109/TMTT.2014.2309637.
21. Parment, F.; Ghiotto, A.; Vuong, T.P.; Duchamp, J.M.; Wu, K. Broadband transition from dielectric-filled to air-filled Substrate Integrated Waveguide for low loss and high power handling millimeter-wave Substrate Integrated Circuits. 2014 IEEE MTT-S International Microwave Symposium (IMS2014), 2014, pp. 1–3. doi:10.1109/MWSYM.2014.6848524.
22. Jin, L.; Lee, R.M.A.; Robertson, I. Analysis and Design of a Novel Low-Loss Hollow Substrate Integrated Waveguide. *IEEE Transactions on Microwave Theory and Techniques* **2014**, *62*, 1616–1624. doi:10.1109/TMTT.2014.2328555.
23. Bigelli, F.; Mencarelli, D.; Farina, M.; Venanzoni, G.; Scalmati, P.; Renghini, C.; Morini, A. Design and Fabrication of a Dielectricless Substrate-Integrated Waveguide. *IEEE Transactions on Components, Packaging and Manufacturing Technology* **2016**, *6*, 256–261. doi:10.1109/TCPMT.2015.2513077.

24. Jastram, N.; Filipovic, D.S. PCB-Based Prototyping of 3-D Micromachined RF Subsystems. *IEEE Transactions on Antennas and Propagation* **2014**, *62*, 420–429. doi:10.1109/TAP.2013.2287899.
25. Belenguer, A.; Borja, A.L.; Esteban, H.; Boria, V.E. High-Performance Coplanar Waveguide to Empty Substrate Integrated Coaxial Line Transition. *IEEE Transactions on Microwave Theory and Techniques* **2015**, *63*, 4027–4034. doi:10.1109/TMTT.2015.2496271.
26. Borja, A.L.; Belenguer, A.; Esteban, H.; Boria, V.E. Design and Performance of a High- $Q$ Narrow Bandwidth Bandpass Filter in Empty Substrate Integrated Coaxial Line at $K_u$ -Band. *IEEE Microwave and Wireless Components Letters* **2017**, *27*, 977–979. doi:10.1109/LMWC.2017.2750118.
27. Arnedo, I.; Arregui, I.; Lujambio, A.; Chudzik, M.; Laso, M.A.G.; Lopetegi, T. Synthesis of Microwave Filters by Inverse Scattering Using a Closed-Form Expression Valid for Rational Frequency Responses. *IEEE Transactions on Microwave Theory and Techniques* **2012**, *60*, 1244–1257. doi:10.1109/TMTT.2012.2187921.
28. Arnedo, I.; Arregui, I.; Chudzik, M.; Teberio, F.; Lujambio, A.; Benito, D.; Lopetegi, T.; Laso, M.A.G. Direct and Exact Synthesis: Controlling the Microwaves by Means of Synthesized Passive Components with Smooth Profiles. *IEEE Microwave Magazine* **2015**, *16*, 114–128. doi:10.1109/MMM.2015.2394011.
29. Caballero, E.D.; Roldan, I.; Urrea, V.; Chudzik, M.; Arregui, I.; Arnedo, I.; Belenguer, A. Mapping smooth profile H-plane rectangular waveguide structures to substrate integrated waveguide technology. *Electronics Letters* **2014**, *50*, 1072–1074. doi:10.1049/el.2014.1581.
30. Schwartz, J.D.; Abhari, R.; Plant, D.V.; Azana, J. Design and Analysis of 1-D Uniform and Chirped Electromagnetic Bandgap Structures in Substrate-Integrated Waveguides. *IEEE Transactions on Microwave Theory and Techniques* **2010**, *58*, 1858–1866. doi:10.1109/TMTT.2010.2050025.
31. Arnedo, I.; Laso, M.A.G.; Falcone, F.; Benito, D.; Lopetegi, T. A Series Solution for the Single-Mode Synthesis Problem Based on the Coupled-Mode Theory. *IEEE Transactions on Microwave Theory and Techniques* **2008**, *56*, 457–466. doi:10.1109/TMTT.2007.914628.
32. Wadell, B.C. *Transmission line design handbook*; Artech House, 1991.
33. Nelder, J.A.; Mead, R. A simplex method for function minimization. *The computer journal* **1965**, *7*, 308–313.